

# Low-Cost Localization for Multihop Heterogeneous Wireless Sensor Networks

Ahmad El Assaf, *Student Member, IEEE*, Slim Zaidi, *Member, IEEE*, Sofiène Affes, *Senior Member, IEEE*, and Nahi Kandil

**Abstract**—In this paper, we propose a novel low-cost localization algorithm tailored for multihop heterogeneous wireless sensor networks (HWSNs) where nodes' transmission capabilities are different. This characteristic, if not taken into account when designing the localization algorithm, may severely hinder its accuracy. Assuming different nodes' transmission capabilities, we develop two different approaches to derive the expected hop progress (EHP). Exploiting the latter, we propose a localization algorithm that is able to accurately locate the sensor nodes owing to a new low-cost implementation. Furthermore, we develop a correction mechanism, which complies with the heterogeneous nature of wireless sensor networks (WSNs) to further improve localization accuracy without incurring any additional costs. Simulations results show that the proposed algorithm, whether applied with or without correction, outperforms in accuracy the most representative WSN localization algorithms.

**Index Terms**—Heterogeneous wireless sensor networks (WSNs), multihop, localization, low cost, energy harvesting (EH), (EH-WSNs), expected hop progress (EHP).

## I. INTRODUCTION

RECENT advances in wireless communications and low-power circuits technologies have led to proliferation of wireless sensor networks (WSNs). A WSN is a set of small and low-cost sensor nodes often equipped with small batteries. The latter are often deployed in a random fashion to sense or collect from the surrounding environments some physical phenomena such as temperature, light, pressure, etc. [1]–[4]. Since power is a scarce resource in such networks, sensor nodes usually recur to multi-hop transmission in order to send their gathered data to an access point (AP). However, the received data at the latter are often fully or partially meaningless if the location from where they have been measured is unknown [5]–[7], making the nodes' localization an essential task in multi-hop WSNs. Owing to the low-cost requirements of WSNs, unconventional paradigms in localization must yet be investigated. Many interesting solutions exist in the literature [8]–[36]. To properly localize each regular or position-unaware node, most

of these algorithms require the distance between the latter and at least three position-aware nodes called hereafter anchors. Since it is very likely in multi-hop WSNs that some regular nodes be unable to directly communicate with all anchors, the distance between each anchor-regular nodes pair is usually estimated using their shortest path. The latter is obtained by summing the distances between any consecutive intermediate nodes located on the shortest path between the two nodes. Depending on the process used to estimate these distances, localization algorithms may fall into three categories: measurement-based, heuristic, and analytical [8]–[36].

Measurement-based algorithms exploit the measurements of the received signals' characteristics such as the received signal strength (RSS) [8]–[9] or the time of arrival (TOA) [11], etc. Using the RSS measurement, the distance between any sensors' pair could be obtained by converting the power loss due to propagation from a sensor to another based on some propagation laws. Unfortunately, due to the probable presence of noise and interference, the distance's estimate would be far from being accurate, thereby leading to unreliable localization accuracy. Using the TOA measurement, nodes require high-resolution clocks and extremely accurate synchronization between them. While the first requirement may dramatically increase the cost and the size of sensor nodes, the second results in severe depletion of their power due to the additional overhead required by such a process. Furthermore, in the presence of noise and/or multipath, the TOA measurement is severely affected thereby hindering nodes' localization accuracy. As far as heuristic algorithms [12]–[14] are concerned, they also have a major drawback. Indeed, most of these algorithms are based on variations of DV-HOP [12] whose implementation in multi-hop WSNs requires a correction factor derived in a non-localized manner and broadcasted in the network by each anchor. This causes an undesired prohibitive overhead and power consumption, thereby increasing the overall cost of the network.

Popular alternatives, more suitable for multi-hop WSNs, are the analytical algorithms [15]–[36] which evaluate theoretically the distance between any two consecutive intermediate nodes. The latter is in fact locally computable at each node, thereby avoiding unnecessary costs incurred if it is fully or partially computed at other nodes and then broadcasted in the network, such as in heuristic algorithms. In spite of their valuable contributions, the approaches developed so far in [15]–[36] to derive that distance are based on the unrealistic assumption that all nodes have the same transmission capabilities (i.e., the WSN is homogenous). However, due to the fact that these sensor

Manuscript received October 15, 2014; revised August 4, 2015; accepted August 13, 2015. Date of publication September 1, 2015; date of current version January 7, 2016. This paper was presented in part at IEEE WCNC 2014 [43]. The associate editor coordinating the review of this paper and approving it for publication was Prof. Andrea Giorgetti.

A. E. Assaf and S. Zaidi are with INRS-EMT, Montreal H5A 1K6, QC, Canada (e-mail: elassaf@emt.inrs.ca; zaidi@emt.inrs.ca).

S. Affes and N. Kandil are with INRS-EMT, Montreal H5A 1K6, QC, Canada, and also with LRTCS-UQAT, Rouyn-Noranda J9P 1Y3, QC, Canada (e-mail: affes@emt.inrs.ca; nahi.kandil@uqat.ca).

Color versions of one or more of the figures in this paper are available online at <http://ieeexplore.ieee.org>.

Digital Object Identifier 10.1109/TWC.2015.2475255

nodes are designed using various technologies to achieve different tasks, their sensing as well as transmission capabilities are very often different. Furthermore, if an energy harvesting (EH) technology is locally integrated at each node, which is the case in the most recently developed WSNs referred to hereafter as EH-WSNs [38]–[42], the available harvested power at nodes would then be random. This phenomenon actually results in the randomization of the nodes' transmission capabilities, since the latter are closely related to the nodes' available powers. During the localization process, it is then very likely that nodes' transmission capabilities be different. As the approaches in [15]–[36] assume the same transmission capability throughout the network, their localization accuracy substantially deteriorates in the so-called heterogeneous WSNs (HWSNs) making them unsuitable for such networks. To the best of our knowledge, there is no analytical algorithm that accounts so far for the heterogeneous nature of WSNs.

To bridge this gap, we propose in this paper a novel analytical algorithm tailored for multi-hop HWSNs where nodes have different transmission capabilities. Taking into account this characteristic, two approaches are developed to accurately derive the distances between any consecutive nodes. Using the so-obtained distances, the proposed algorithm is able to accurately locate the nodes owing to a new low-cost implementation. Furthermore, we develop a correction mechanism which complies with the heterogeneous nature of WSNs to further improve localization accuracy without incurring any additional costs. Simulations results show that the proposed algorithm, whether applied with or without correction, outperforms in accuracy the most representative multi-hop WSNs localization algorithms.

The rest of this paper is organized as follows: Section II describes the system model and discusses the motivation of this work. Section III derives the distance between consecutive sensors using two approaches. A novel localization algorithm for HWSNs is proposed in section IV. Its implementation cost is discussed in Section VI. Simulation results are discussed in Section VII and concluding remarks are made in section VIII.

*Notation:* Uppercase and lowercase bold letters denote matrices and vectors, respectively.  $[\cdot]_{il}$  and  $[\cdot]_i$  are the  $(i, l)$ -th entry of a matrix and  $i$ -th entry of a vector, respectively.  $\mathbf{I}$  is the identity matrix.  $(\cdot)^T$  denotes the transpose.  $D(i, x)$  denotes the disc having the  $i$ -th sensor as a center and  $x$  as a radius.

## II. NETWORK MODEL AND OVERVIEW

Fig. 1 illustrates the system model of  $N$  sensor nodes uniformly deployed in a 2-D square area  $S$ . The transmission coverage of each node is assumed to be circular, i.e., the  $i$ -th node could directly communicate with any node located in  $D(i, Tc_i)$ , the disc having this node as a center and its transmission capability  $Tc_i$  as a radius [37]. In a multi-hop transmission, note that the  $i$ -th node could also communicate with any node located outside its coverage area  $D(i, Tc_i)$ . Due to the heterogenous nature of WSNs, nodes are assumed here to have different transmission capabilities. It is also assumed that only a few nodes commonly known as anchors are aware of their positions. The other nodes, called hereafter position-unaware

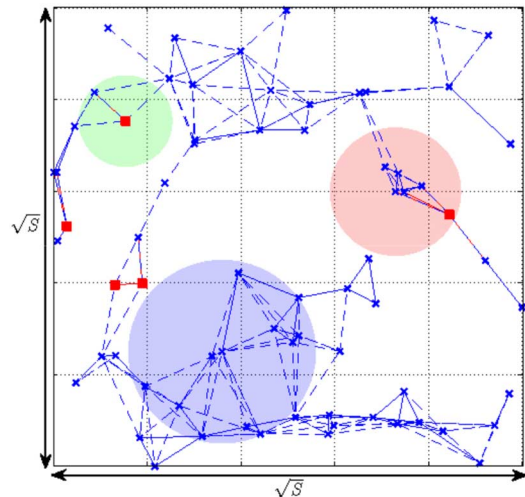


Fig. 1. Network model.

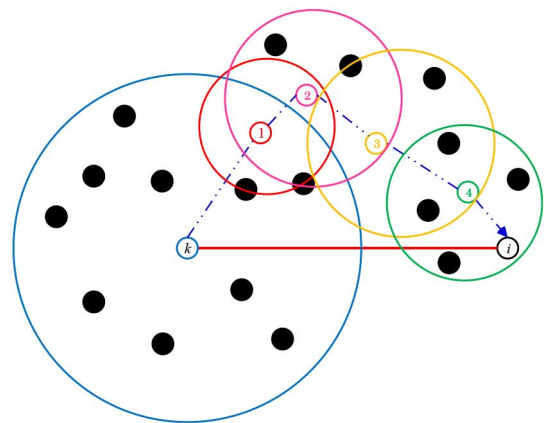


Fig. 2. Multi-hop transmission.

or regular nodes for the sake of simplicity, are oblivious to this information. As shown in Fig. 1, the anchors are marked with red squares and the regular nodes are marked with blue crosses. If a node is located within the coverage area of another node, the two nodes are linked with a dashed line that represents one hop. Three discs were drawn as few illustrative examples of the coverage areas of the corresponding nodes. Let  $N_a$  and  $N_u = N - N_a$  denote the number of anchors and regular nodes, respectively. Without loss of generality, let  $(x_i, y_i)$ ,  $i = 1, \dots, N_a$  be the coordinates of the anchors and  $(x_i, y_i)$ ,  $i = N_a + 1, \dots, N$  those of the regular nodes.

As a first step of any localization algorithm for multi-hop WSNs aiming to estimate the regular nodes' positions, the  $k$ -th anchor broadcasts through the network a message containing its position. As it can be seen in Fig. 2, if the  $(i - N_a)$ -th regular node (or the  $i$ -th node) is located outside the anchor coverage area, it receives this message through multi-hop transmission. For simplicity, let us assume that only one intermediate node  $j$  located over the shortest path between the  $k$ -th anchor and the  $i$ -th node is necessary (i.e., two-hop transmission). Assuming a high node density in the network, the distance  $d_{k-i}$  between the two nodes can be accurately approximated as [15]–[36]

$$d_{k-i} \simeq d_{k-j} + d_{j-i}, \quad (1)$$

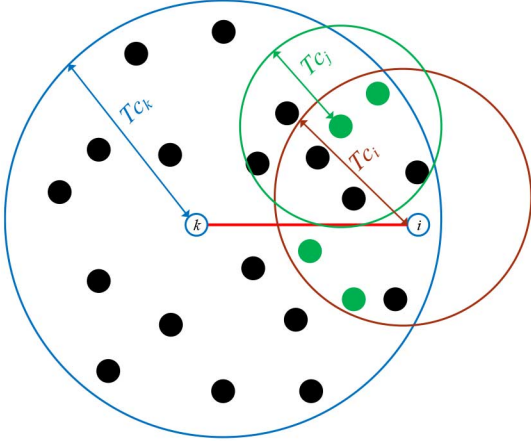


Fig. 3. Node's neighborhood in HWSN.

where  $d_{k-j}$  ( $d_{j-i}$ ) is the effective distance between the  $k$ -th ( $i$ -th) and  $j$ -th nodes. Two methods have been so far developed to analytically estimate the distance  $d_{k-i}$  exploiting the aforementioned approximation [15]–[36]. In the first method, the  $j$ -th node estimates the distance  $d_{k-j}$  using the number of common neighbors with the  $k$ -th node. In fact, if  $n_{kj}$  common neighbors exist in the intersection area  $I = D(k, Tc_k) \cap D(j, Tc_j)$ ,  $I$  could be approximated by  $\hat{I} = n_{kj}\lambda^{-1}$  where  $\lambda = N/S$  is the average node density in the network. Furthermore, using some geometrical properties, one can show that

$$I = f(d_{k-j}) = Tc_j^2 \cos^{-1} \left( \frac{d_{k-j}^2 + Tc_j^2 - Tc_k^2}{2d_{k-j}Tc_j} \right) + Tc_k^2 \cos^{-1} \left( \frac{d_{k-j}^2 + Tc_k^2 - Tc_j^2}{2d_{k-j}Tc_k} \right) - \frac{1}{2} \sqrt{4d_{k-j}^2 Tc_k^2 - (d_{k-j}^2 - Tc_j^2 + Tc_k^2)^2}. \quad (2)$$

$d_{k-j}$  is then obtained as  $d_{k-j} = f^{-1}(I) \simeq f^{-1}(n_{kj}\lambda^{-1})$ . Since it is impossible to derive  $f^{-1}$  in closed-form,  $d_{k-j}$  can be numerically derived using for instance the well-known secant method. The problem here is that the  $j$ -th node needs to be aware of  $n_{kj}$  to be able to estimate the area  $I$ . To this end, the  $k$ -th and  $j$ -th nodes broadcast a “Hello” message that will be sent back by their respective neighbors. Upon reception of the  $k$ -th node neighbors’ list, the  $j$ -th node compares it with its own neighbors’ list and, hence,  $n_{kj}$  is obtained. Unfortunately, it is no longer possible to get an exact knowledge of  $n_{kj}$  in HWSNs. Indeed, in such networks, it is very likely that the neighbor of a node has a different transmission capability from the latter. Thus, as shown in Fig. 3, some “Hello” messages sent back by some respective neighbors of the  $k$ -th and  $j$ -th node would not reach the latter nodes, due to their weaker capabilities. Consequently, the  $j$ -th node obtains  $\hat{n}_{kj} \leq n_{kj}$  leading, hence, to inaccurate distance estimation. Note that this discussion also holds for  $d_{j-i}$ . This proves that this first analytical method is not suitable for HWSNs.

The second method uses the fact that the minimum mean square error (MMSE) of the distance estimation is obtained if  $\hat{d} = E(d)$  and, hence,

$$\hat{d}_{k-i} \simeq \bar{d}_{k-j} + \bar{d}_{j-i}, \quad (3)$$

where  $\bar{d}_{k-j} = E\{d_{k-j}\}$  is the expected hop progress (EHP) and  $\bar{d}_{j-i} = E\{d_{j-i}\}$  is the mean last hop (MLH). One of the well-known analytical expressions of EHP is the one developed in [23] as follows:

$$\bar{d}_{k-j} = \sqrt{3}\lambda \int_0^{Tc_k} x^2 e^{-\frac{1}{3}\lambda\pi(Tc_k^2 - x^2)} dx, \quad (4)$$

where  $\lambda$  is the node density, and  $x$  is the distance between the  $k$ -th and the  $i$ -th node. From (4), the EHP a priori depends only on the  $k$ -th node transmission capability  $Tc_k$  and, therefore, its computation does not supposedly require any knowledge of the  $j$ -th node transmission capability  $Tc_j$ . In what follows, and in contrast to (4), we will prove the EHP expression to be dependent on both  $Tc_k$  and  $Tc_j$  thereby revealing the expression derived in [23], as one example among too many others [20]–[28] whose approaches are similar to the above but not discussed here for lack of space, to lack accuracy.

Let  $F$  be the potential forwarding area wherein the intermediate node  $j$  could be located. Since this node should, at the same time, be located in the  $k$ -th node coverage area and communicate directly with the  $i$ -th node using its transmission capability  $Tc_j$ ,  $F$  is given by

$$F = D(k, Tc_k) \cap D(i, Tc_j). \quad (5)$$

It is noteworthy that the EHP is nothing but the mean of all distances between the  $k$ -th node and all the potential intermediate nodes located in  $F$  and, hence, the EHP strongly depends on  $F$ . As can be observed from Fig. 4, if the intermediate node transmission capability  $Tc_j$  increases, the potential forwarding area  $F$  increases to include potential intermediate nodes closer to the  $k$ -th anchor, thereby decreasing the EHP. Likewise, if  $Tc_j$  decreases,  $F$  decreases to exclude potential intermediate nodes closer to the  $k$ -th anchor and, hence, the EHP increases. Consequently, the EHP depends not only on  $Tc_k$ , but also on  $Tc_j$ . Let us now turn our attention to the MLH. It is obvious that the transmission capability of the  $i$ -th node does not have any effects on the last hop size  $d_{j-i}$ . Therefore, in contrast with the EHP, the MLH depends only on the transmission capability of the transmitting node  $j$ . In the next section, novel approaches are developed to accurately derive the expressions of both the MLH and the EHP. These results will be exploited in Section IV to propose a low-cost localization algorithm that complies with the heterogeneous nature of WSNs.

### III. ANALYTICAL EVALUATION OF THE MLH AND EHP

In this section, expressions of both the MLH and the EHP are accurately derived. To this end, we consider the same scenario described in Section II. For the sake of clarity, in what follows, we denote by  $X$ ,  $Y$ , and  $Z$  the random variables that represent  $d_{k-i}$ ,  $d_{j-i}$ , and  $d_{k-j}$ , respectively.

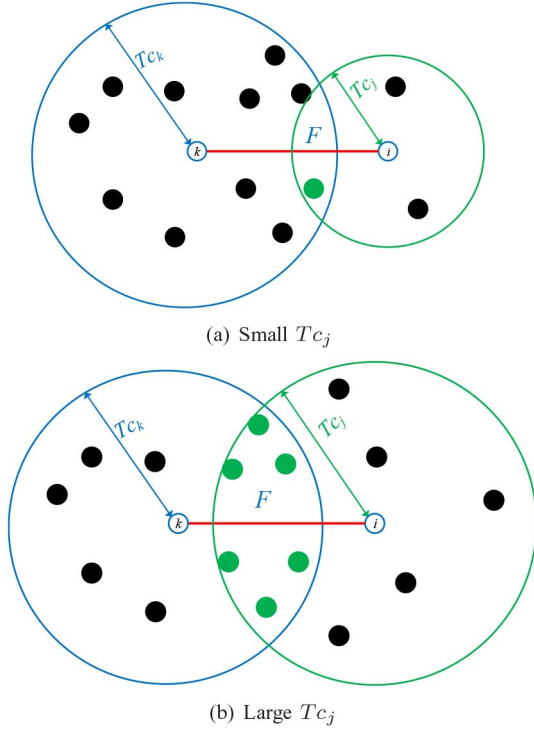


Fig. 4. Effect of the intermediate node transmission capability.

#### A. MLH derivation

Since the  $i$ -th regular node could be located anywhere in  $D(j, Tc_j)$  (the  $j$ -th node's coverage area) with the same probability,  $Y$  can be considered as a uniformly<sup>11</sup> distributed random variable on  $[0, Tc_j]$ . Therefore, the MLH denoted hereafter by  $h_{\text{last}}(Tc_j)$  is given by

$$h_{\text{last}}(Tc_j) = \int_0^{Tc_j} y f_Y(y) dy = \int_0^{Tc_j} \frac{y}{Tc_j} dy = \frac{Tc_j}{2}, \quad (6)$$

where  $f_Y(y) = 1/Tc_j$  is the probability density function (pdf) of  $Y$ .

#### B. EHP derivation

In order to derive the EHP, one should first compute the conditional cumulative distribution function (CDF)  $F_{Z|X}(z) = P(Z \leq z|x)$  of  $Z$  with respect to the random variable  $X$ . In the following, two approaches are proposed to derive this CDF.

1) *Approach 1:* As can be shown from Fig. 5,  $Z \leq z$  is guaranteed only if there are no nodes in the dashed area  $A$ . Therefore, the conditional CDF  $F_{Z|X}(z)$  can be defined as

$$F_{Z|X}(z) = P(Z \leq z|x) = P(A_0|F_1), \quad (7)$$

where  $P(A_0|F_1)$  is the probability that the event  $A_0 = \{\text{no nodes in the dashed area } A\}$  given  $F_1 = \{\text{at least one node in the potential forwarding area}\}$  occurs. Since the nodes are uniformly deployed in  $S$ , the probability of having  $K$  nodes in  $F$

<sup>11</sup>This assumption is actually made to simplify the analytical derivations, thereby reducing the computational burden at each node.

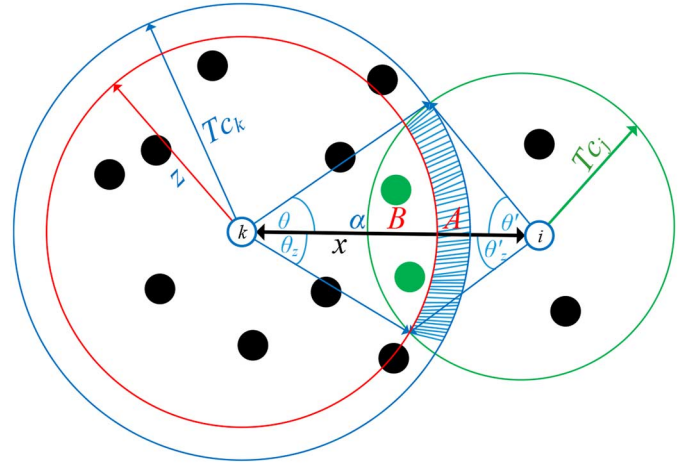


Fig. 5. EHP analysis.

follows a Binomial distribution  $\text{Bin}(N, p)$  where  $p = \frac{F}{S}$ . For relatively large  $N$  and small  $p$ , it can be readily shown that  $\text{Bin}(N, p)$  can be accurately approximated by a Poisson distribution  $\text{Pois}(\lambda F)$  [30]. Using the Bayes' theorem,  $F_{Z|X}(z)$  could be rewritten as

$$F_{Z|X}(z) = \frac{P(F_1|A_0) P(A_0)}{P(F_1)}, \quad (8)$$

and, hence, for a large number of nodes  $N$  and small  $p$ , we have

$$F_{Z|X}(z) = \frac{e^{-\lambda A} (1 - e^{-\lambda B})}{(1 - e^{-\lambda F})}, \quad (9)$$

where  $B = F - A$ . In the equation above, note that we use the fact that  $P(F_1|A_0)$  is the probability that at least one node is in  $B$ . As can be observed from (9), when  $z = \alpha$  where  $\alpha = x - Tc_j$ , we have  $B = 0$  and  $A = F$  and, therefore,  $F_{Z|X}(z) = 0$ . This is expected since all potential intermediate nodes are located in the forwarding zone  $F$  where any node is at least at distance  $\alpha$  from the  $k$ -th node (i.e.,  $P(Z \leq \alpha) = 0$ ). Furthermore, if  $z = Tc_k$ , it holds that  $B = F$  and  $A = 0$  and, hence,  $P(Z \leq Tc_k) = 1$ . This is also expected since all potential intermediate nodes are located in the  $k$ -th node's coverage area at distance  $Tc_k$  at most from the latter (i.e.,  $P(Z \leq Tc_k) = 1$ ). It should be noticed here that the properties above are not satisfied by any previously developed CDF expressions such as those in [23]–[24].

Using some geometrical properties and trigonometric transformations, one can readily show that

$$F = Tc_k^2 \left( \theta - \frac{\sin(2\theta)}{2} \right) + Tc_j^2 \left( \theta' - \frac{\sin(2\theta')}{2} \right), \quad (10)$$

$$B = z^2 \left( \theta_z - \frac{\sin(2\theta_z)}{2} \right) + Tc_j^2 \left( \theta'_z - \frac{\sin(2\theta'_z)}{2} \right), \quad (11)$$

where  $\theta = \arccos\left(\frac{Tc_k^2 - Tc_j^2 + x^2}{2Tc_k x}\right)$ ,  $\theta' = \arccos\left(\frac{Tc_j^2 - Tc_k^2 + x^2}{2Tc_j x}\right)$ ,  $\theta_z = \arccos\left(\frac{z^2 - Tc_j^2 + x^2}{2zx}\right)$ , and  $\theta'_z = \arccos\left(\frac{Tc_j^2 - z^2 + x^2}{2Tc_j x}\right)$ .

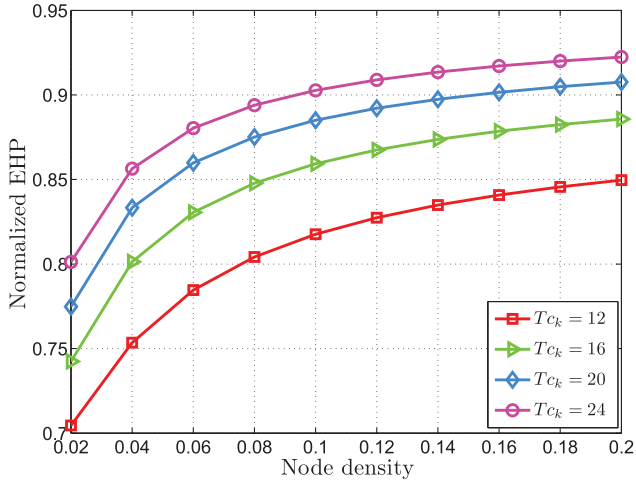


Fig. 6. Effect of the  $k$ -th node transmission capability on the EHP.

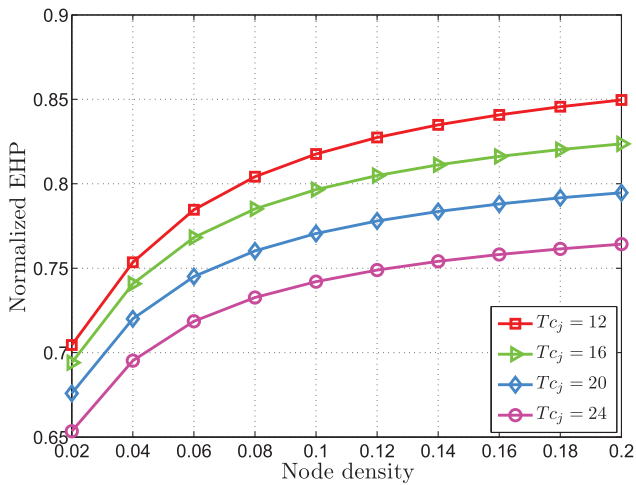


Fig. 7. Effect of the intermediate node transmission capability on the EHP.

Finally, the EHP  $h(Tc_k, Tc_j)$  between the  $k$ -th and  $j$ -th nodes can be derived as

$$\begin{aligned} h(Tc_k, Tc_j) &= \mathbb{E}_x \left( \alpha H_{Z|X}(\alpha) + \int_{\alpha}^{Tc_k} H_{Z|X}(z) dz \right) \\ &= \int_{Tc_k}^{Tc_k+Tc_j} \left( \alpha H_{Z|X}(\alpha) + \int_{\alpha}^{Tc_k} H_{Z|X}(z) dz \right) f_X(x) dx, \end{aligned} \quad (12)$$

where  $H_{Z|X}(z) = 1 - F_{Z|X}(z)$  and  $f_X(x)$  is the pdf of  $X$ . Note that the latter can be considered as a Uniform<sup>1</sup> random variable over  $[Tc_k, Tc_k + Tc_j]$  and, hence,  $f_X(x)$  can be substituted there by  $1/Tc_j$ . To the best of our knowledge, a closed-form expression for the EHP in (12) does not exist. However,  $h(Tc_k, Tc_j)$  can be easily implemented since it depends on finite integrals. As can be observed from (12), the proposed EHP depends on both  $Tc_k$  and  $Tc_j$ . Such extremely important and crucial features in HWSNs no longer hold true for the previously proposed EHPs, such as in (4), which are only dependent on the sender node's transmission capability. It can be shown from Figs. 6 and 7 that the so-obtained EHP decreases if  $Tc_j$

increases while it increases when  $Tc_k$  increases. This collaborates the discussion made above. These figures also show that the proposed EHP above increases with the node density. This is expected since it is very likely that the per-hop distance increases when the number of nodes located in  $F$  increases if, of course, both  $Tc_k$  and  $Tc_j$  are fixed. Therefore, the so-obtained EHP expression is more accurate than those developed so far and, hence, should allow more accurate distance estimation and more reliable localization as will be shown next.

2) *Approach 2:* The main issue with the approach developed above is that it holds only when the number of nodes  $N$  is sufficiently large and the area  $F$  is much smaller than the network size. Since  $N$  is typically large in the context of WSNs, the first condition is very likely to be satisfied. Unfortunately, the second condition cannot be always guaranteed, especially when the transmission capabilities  $Tc_k$  and  $Tc_j$  are not small enough. Indeed, in such a case  $F$  is very likely to be large and, hence, the EHP derived using the above CDF is no longer accurate. In this section, we propose another approach aiming to derive this CDF for any  $N$ ,  $Tc_k$  and  $Tc_j$ .

Let us assume that  $M$  potential intermediate nodes exist between the  $i$ -th and  $k$ -th nodes, or, in other words,  $M$  potential positions of the intermediate node  $j$  exist in  $F$ . Let  $Z_m$  be the random variable that represents the distance between the  $k$ -th node and the  $m$ -th potential intermediate node. Thus, one can define  $F_{Z|X}(z)$  as follows

$$F_{Z|X}(z) = P(Z_1 \leq z \cap Z_2 \leq z, \dots, \cap Z_M \leq z). \quad (13)$$

Using the fact that  $Z_m, m = 1, \dots, M$  are independently and identically distributed (i.i.d) random variables, we obtain

$$F_{Z|X}(z) = P(Z_m \leq z)^M. \quad (14)$$

As can be observed from Fig. 5, in order to satisfy  $Z_m \leq z$ , the  $m$ -th intermediate node should be located in the area  $B$  and, hence,

$$F_{Z_m|X}(z) = P(Z_m \leq z|x) = P(E_2), \quad (15)$$

where  $P(E_2)$  is the probability that the event  $E_2 = \{\text{the } m\text{-th intermediate node is located in } B\}$  occurs. Since the nodes distribution is assumed to be uniform, the  $m$ -th intermediate node could be located anywhere in  $F$  with the same probability. Therefore, the probability that this node is located in any area  $\Omega \subset F$  is nothing but the ratio of  $\Omega$  to  $F$ . Consequently,  $F_{Z|X}(z)$  is given by

$$F_{Z|X}(z) = \left(1 - \frac{A}{F}\right)^M. \quad (16)$$

Using similar steps to derive  $A$ , it can be shown that

$$F = Tc_k^2 \left( \theta - \frac{\sin(2\theta)}{2} \right) + Tc_j^2 \left( \theta' - \frac{\sin(2\theta')}{2} \right), \quad (17)$$

where  $A$  is obtained by subtracting (11) from (10). Finally, the EHP is derived by substituting (16) in (12). By avoiding the Binomial-to-Poisson approximation exploited in Approach 1,

the obtained EHP using Approach 2 is then valid for any  $N$ ,  $T_{c_k}$  and  $T_{c_j}$  and, hence, it is more likely to be accurate than that developed in Section III-B1. However, the main drawback of Approach 2 is that the EHP depends on the number of potential intermediate nodes  $M$  which should be determined by training, i.e., at additional overhead and power costs with respect to Approach 1. Therefore, the latter should be employed when the power and overhead costs' restrictions are severe while Approach 2, which performs better as will be verified later by simulations in Section VII, should be used if these restrictions are alleviated.

In the next section, based on the so-obtained EHP and MLH expressions, we propose a novel localization algorithm suitable for HWSNs where nodes have different range capabilities.

#### IV. PROPOSED LOCALIZATION FOR HWSNS

In this section, we propose a novel three-step localization algorithm for HWSNs. In the first step, the regular nodes receive in a multi-hop fashion all the information required to estimate their respective positions while, in the second step, they compute an initial guess exploiting one of the two EHP expressions developed above. In the third and last step, a correction mechanism is locally performed at each node, in order to further minimize the incurred localization errors. These three steps will be further detailed in the sequel.

##### A. Initialization

In this step, the  $k$ -th anchor starts by broadcasting through the network a packet which consists of a header followed by a data payload. The packet header contains the anchor position  $(x_k, y_k)$ , while the data payload contains  $(T_{c_k}, \hat{d}_k)$ , where  $T_{c_k}$  is the transmission capability of the  $k$ -th anchor and  $\hat{d}_k$  is the estimated distance initialized to zero. If the packet is successfully received by a node, the latter estimates the EHP using either Approach 1 or 2 above, adds it to  $\hat{d}_k$ , stores the resulting value in its database and then, rebroadcasts the resulting packet after substituting  $T_{c_k}$  by its own transmission capability. Once this packet is received by another node, its database information is checked. If the  $k$ -th anchor information exists and the stored estimated distance is larger than that of the received one, the node updates the  $k$ -th anchor's information, then broadcasts the resulting packet after substituting the received transmission capability by its own. Otherwise, the node discards the received packet. However, when the node is oblivious to the  $k$ -th anchor position, it adds this information to its database and forwards the received packet after substituting the received transmission capability by its own. This mechanism will continue until each regular node in the network becomes aware of each anchor position as well as the distance from the latter to the last intermediate node before reaching that node. Note that the implementation of the proposed algorithm requires that each node broadcasts the anchor information not only with its estimated distance but also its transmission capability to allow the EHP computation at the next receiving node. In contrast, the

implementation of existing algorithms in HWSNs requires the broadcast of the anchor information and the estimated distance only. Yet we will prove next in Section VI that the additional power cost that could be incurred a priori when broadcasting the transmission capabilities can be easily avoided by the proposed algorithm.

##### B. Positions' computation

In this section, we will show how the so-received information can be exploited to get an initial guess of each regular node position. Using its available information, the  $(i - N_a)$ -th regular node (or the  $i$ -th node) computes an estimate of its distance to the  $k$ -th anchor as

$$\hat{d}_{k-i} = \hat{d}_k + h_{\text{last}}(T_{c_{k+L}}), \quad (18)$$

where

$$\hat{d}_k = \sum_{l=k}^{k+L-1} h(T_{c_l}, T_{c_{l+1}}), \quad (19)$$

is the distance from the  $k$ -th anchor to the last intermediate node. In (18) and (19), we assume for simplicity, yet without loss of generality, that  $L$  intermediate nodes exist over the shortest path between the  $k$ -th anchor and the  $(i - N_a)$ -th regular node and that the  $l$ -th intermediate node is the  $(k + l)$ -th node. Using its estimated distances to the  $N_a$  anchors as well as the latter's coordinates, the position of the  $(i - N_a)$ -th regular node could be obtained by multilateration [45].

Unfortunately, errors are expected to occur when estimating the distance between each regular node-anchor pair, thereby hindering localization accuracy. As a third step of our proposed algorithm, we propose a correction mechanism aiming to reduce this error.

##### C. Correction mechanism

Let  $\epsilon_{ki}$  denote the estimation error of the distance between the  $k$ -th anchor and the  $i$ -th regular node as

$$\epsilon_{ki} = \hat{d}_{k-i} - d_{k-i}, \quad (20)$$

where  $d_{k-i}$  is the true distance between the two nodes. As discussed above, this error hinders localization accuracy. As such, we have

$$\begin{cases} x_i = \hat{x}_i + \delta_{x_i} \\ y_i = \hat{y}_i + \delta_{y_i} \end{cases}, \quad (21)$$

where  $\delta_{x_i}$  and  $\delta_{y_i}$  are the location coordinates' errors to be determined. Exploiting the Taylor series expansion and retaining the first two terms, the following approximation holds:

$$d_{k-i} \simeq \tilde{d}_{k-i} + \psi_{ki} \delta_{x_i} + \phi_{ki} \delta_{y_i}, \quad (22)$$

where

$$\tilde{d}_{k-i} = \sqrt{(\hat{x}_i - x_k)^2 - (\hat{y}_i - y_k)^2}, \quad (23)$$

and

$$\psi_{ki} = \frac{\partial \tilde{d}_{k-i}}{\partial x} \Big|_{\hat{x}_i, \hat{y}_i} = \frac{\hat{x}_i - x_k}{\sqrt{(\hat{x}_i - x_k)^2 - (\hat{y}_i - y_k)^2}} = \frac{\hat{x}_i - x_k}{\tilde{d}_{k-i}}, \quad (24)$$

$$\phi_{ki} = \frac{\partial \tilde{d}_{k-i}}{\partial y} \Big|_{\hat{x}_i, \hat{y}_i} = \frac{\hat{y}_i - y_k}{\sqrt{(\hat{x}_i - x_k)^2 - (\hat{y}_i - y_k)^2}} = \frac{\hat{y}_i - y_k}{\tilde{d}_{k-i}}, \quad (25)$$

for  $k = 1, 2, \dots, N_a$ . Note that  $\tilde{d}_{k-i}$  is different from  $\hat{d}_{k-i}$  due to the error incurred by multilateration [45]. Therefore, rewriting (22) in a matrix form yields

$$\mathbf{\Gamma}_i \boldsymbol{\delta}_i = \boldsymbol{\zeta}_i - \boldsymbol{\epsilon}_i, \quad (26)$$

where  $\mathbf{\Gamma}$  is a  $N_a \times 2$  matrix with

$$[\mathbf{\Gamma}_i]_{k1} = \psi_{ki}, [\mathbf{\Gamma}_i]_{k2} = \phi_{ki}, \quad (27)$$

and

$$\boldsymbol{\zeta}_i = [\hat{d}_{i-1} - \tilde{d}_{i-1} \quad \hat{d}_{i-2} - \tilde{d}_{i-2} \dots \hat{d}_{i-N_a} - \tilde{d}_{i-N_a}]^T, \quad (28)$$

$$\boldsymbol{\epsilon}_i = [\epsilon_{1i}, \epsilon_{2i}, \dots, \epsilon_{N_a i}]^T, \text{ and } \boldsymbol{\delta}_i = [\delta_{x_i}, \delta_{y_i}]^T.$$

---

#### Algorithm 1. Proposed algorithm for every nodes

---

**Input:** Number of anchors  $N_a$ , and their positions  $(x_k, y_k)$ , where  $k = 1, \dots, N_a$ , as well as their transmission capabilities

**for**  $i = 1 \rightarrow N_a$  **do**

$\hat{d}_{k-i} \leftarrow$  using Approach 1 or 2 (Section III)

**end for**

$\hat{x}_i, \hat{y}_i \leftarrow$  Multilateration

$$\boldsymbol{\delta}_i = \left( \mathbf{\Gamma}_i^T \mathbf{P}_i^{-1} \mathbf{\Gamma}_i \right)^{-1} \mathbf{\Gamma}_i^T \mathbf{P}_i^{-1} \boldsymbol{\zeta}_i \leftarrow \text{Eq. (29)}$$

$$x_i \leftarrow \hat{x}_i + \delta_x;$$

$$y_i \leftarrow \hat{y}_i + \delta_y;$$

**while**  $\delta_i \geq 0$  **do**

$$\hat{x}_i \leftarrow x_i;$$

$$\hat{y}_i \leftarrow y_i;$$

Recalculate  $|\delta_i| \leftarrow$  Eq. (29)

$$x_i \leftarrow \hat{x}_i + \delta_x;$$

$$y_i \leftarrow \hat{y}_i + \delta_y;$$

**end while**

**Output**  $(x_i, y_i)$  ▷ Estimated position of the  $i$ -th node

---

Many methods such as the weighted least squares (WLS) might be used to properly derive  $\boldsymbol{\delta}_i$ . Using WLS, the solution of (26) is given by :

$$\boldsymbol{\delta}_i = \left( \mathbf{\Gamma}_i^T \mathbf{P}_i^{-1} \mathbf{\Gamma}_i \right)^{-1} \mathbf{\Gamma}_i^T \mathbf{P}_i^{-1} \boldsymbol{\zeta}_i, \quad (29)$$

where  $\mathbf{P}_i$  is the covariance matrix of  $\boldsymbol{\epsilon}_i$ . Since  $\epsilon_{ki}$   $k = 1, \dots, N_a$  are independent random variables,  $\mathbf{P}_i$  boils down to  $\text{diag} \{ \sigma_{1i}^2, \dots, \sigma_{N_a i}^2 \}$  where  $\sigma_{ki}^2$  is the variance of  $\epsilon_{ki}$ . A straightforward inspection of (29) reveals that  $\boldsymbol{\delta}_i$  depends on some

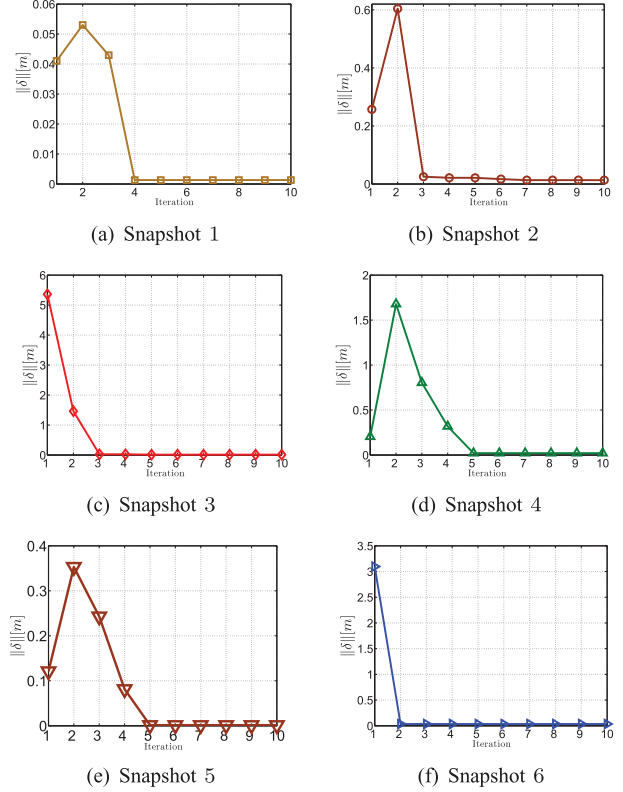


Fig. 8. Convergence of  $|\boldsymbol{\delta}|$  vs. the number of iterations.

locally available information as well as all  $\sigma_{ki}^2, k = 1, \dots, N_a$ . Yet we will show in what follows that the derivation of  $\sigma_{ki}^2, k = 1, \dots, N_a$  requires a negligible additional power cost that could be easily avoided. Once we get  $\boldsymbol{\delta}_i$ , the value of  $(\hat{x}_i, \hat{y}_i)$  is updated as  $\hat{x}_i = \hat{x}_i + \delta_{x_i}$  and  $\hat{y}_i = \hat{y}_i + \delta_{y_i}$ . The computations are repeated until  $|\boldsymbol{\delta}_i|$  approaches zero. In such a case, we have from (21) that  $x_i \simeq \hat{x}_i$  and  $y_i \simeq \hat{y}_i$  and, hence, more accurate localization is performed. As can be observed from Fig. 8, the proposed correction mechanism converges after 5 iterations at most. Nevertheless, we will prove in Section VI that the proposed algorithm perfectly tailored for HWSNs, and whose pseudocode implementable at each node is summarized in Algorithm 1, does not burden the overall cost of the WSN.

## V. VARIANCE EVALUATION

This section aims to derive the expression of the variances  $\sigma_{ki}^2, k = 1, \dots, N_a$  which are required for the proposed algorithm's implementation. As such, two different methods, analytical and non-parametric, are proposed.

### A. Analytical method

Assuming a high node density in the network, the distance  $d_{k-i}$  between two nodes can be rewritten as

$$d_{k-i} \simeq \sum_{l=k}^{k+L} d_{l-(l+1)}, \quad (30)$$

where  $L$  is the number of intermediate nodes over the shortest path and  $d_{l-(l+1)}$  is the distance between the  $l$ -th and  $(l+1)$ -th intermediate node. It follows from (18) and (30) that the distance estimation error (DER)  $\varepsilon_{ki}$  is given by

$$\varepsilon_{ki} \simeq \sum_{l=k}^{k+L-1} e_l + e_{\text{last}}, \quad (31)$$

with  $e_l = h(Tc_l, Tc_{l+1}) - d_{l-(l+1)}$  being the error incurred during the  $(l-k+1)$ -th hop and  $e_{\text{last}} = h_{\text{last}}(Tc_{k+L}) - d_{(k+L)-i}$  the error incurred at the last hop. It can be readily shown from (31) that  $\sigma_{ki}^2 = \sum_{l=k}^{k+L-1} \sigma_l^2 + \sigma_{\text{last}}^2$  where  $\sigma_l^2$  and  $\sigma_{\text{last}}^2$  are the variances of  $e_l$  and  $e_{\text{last}}$ , respectively. Using the results developed in Section III, we obtain

$$\sigma_{\text{last}}^2 = \frac{Tc_{(k+L)}^2}{12}, \quad (32)$$

and

$$\begin{aligned} \sigma_l^2 = & \int_{Tc_l}^{Tc_l+Tc_{l+1}} \left( \alpha^2 H(\alpha) + 2 \int_{\alpha}^{Tc_l} z H(z) dz \right) f_X(x) dx \\ & - \left( \int_{Tc_l}^{Tc_l+Tc_{l+1}} \left( \alpha H(\alpha) + \int_{\alpha}^{Tc_l} H(z) dz \right) f_X(x) dx \right)^2. \end{aligned} \quad (33)$$

Note that  $\sigma_l^2$  could be obtained using any of the CDFs developed in Section III-B. As can be observed from (32) and (33),  $\sigma_{\text{last}}^2$  is locally computable by the  $i$ -th node while  $\sigma_l^2$  should be computed at the  $(l+1)$ -th intermediate node, added to the term  $\sum_{m=k}^{l-1} \sigma_m^2$ , then forwarded to the next intermediate node. This results in additional few bits that must be transmitted by each node in the network. In what follows, we will prove that the additional power cost that could be incurred a priori when transmitting  $\sigma_l$  can be easily avoided by the proposed algorithm.

### B. Non-parametric method

In the previous section, the analytical expression of  $\sigma_{ki}^2$  was derived using the approximation in (30) which holds only for highly dense networks. However, if this assumption is not satisfied (i.e., lowly dense network), (30) would no longer be valid and, hence,  $\sigma_{ki}^2$ 's expression would no longer be accurate enough. In such a case, to properly derive  $\sigma_{ki}^2$ , we propose to exploit the PDF of the DER  $\varepsilon_{ki}$  denoted by  $f(\varepsilon)$ . Unfortunately, to the best of our knowledge, there is no closed form solution for such a PDF. In this work, we propose to use a non-parametric technique to estimate it owing to some potential observations available at anchors. So far, many non-parametric techniques have been proposed in the literature such as the histogram [49] and the well-known kernel density estimation (KDE) [50] techniques. In this paper, we are only concerned by the latter which can estimate an arbitrary distribution without much observations. Such observations can in fact be easily obtained at the  $k$ -th anchor. Indeed, since this anchor is aware of all other anchor positions, it is able to derive the actual distances between it and the latters. Using (18), the

$k$ -th anchor could also obtain the estimated distances between it and the other anchors and, therefore, derive  $\varepsilon_{ki}$ . Hence, if  $N_a$  anchors exist in the network, the total number of available observations is  $n_o = N_a(N_a - 1)$ . Let  $\varepsilon_1, \varepsilon_2, \dots, \varepsilon_{n_o}$  denote such observations. Using the KDE technique,  $f(\varepsilon)$  can be then approximated by

$$\hat{f}(\varepsilon) = \frac{1}{ps_\varepsilon} \sum_{t=1}^{n_o} K\left(\frac{\varepsilon - \varepsilon_t}{s_\varepsilon}\right), \quad (34)$$

where  $s_\varepsilon$  is a smoothing parameter determined using the method in [51] and  $K(\varepsilon)$  is the Gaussian kernel given by

$$K(\varepsilon) = \frac{1}{\sqrt{2\pi}} \exp\left(-\frac{1}{2}\varepsilon^2\right). \quad (35)$$

As can be noticed from (34) and (35), the estimated PDF is computed by averaging the Gaussian density over all observations. Substituting (35) in (34) and using the resulting PDF to compute  $\sigma_{ki}^2$  yields

$$\sigma_{ki}^2 = \frac{\sum_{t=1}^{n_o} (X_t G_t - Y_t^2)}{\sum_{t=1}^{n_o} G_t^2}, \quad (36)$$

where

$$\begin{aligned} X_t = & \left( s_\varepsilon^2 + \varepsilon_t^2 \right) G_t - s_\varepsilon^2 \left( (\varepsilon_t + 1) e^{-\frac{(1-\varepsilon_t)^2}{2s_\varepsilon^2}} \right. \\ & \left. + (\varepsilon_t - 1) e^{-\frac{(1+\varepsilon_t)^2}{2s_\varepsilon^2}} \right), \end{aligned} \quad (37)$$

$$G_t = s_\varepsilon \sqrt{2\pi} \left( Q\left(\frac{\varepsilon_t - 1}{s_\varepsilon}\right) - Q\left(\frac{\varepsilon_t + 1}{s_\varepsilon}\right) \right), \quad (38)$$

and

$$Y_t = \varepsilon_t G_t - s_\varepsilon^2 \left[ e^{-\frac{(1-\varepsilon_t)^2}{2s_\varepsilon^2}} - e^{-\frac{(1+\varepsilon_t)^2}{2s_\varepsilon^2}} \right], \quad (39)$$

with  $Q(x)$  being the Q-function.

Fig. 9 plots the empirical  $f(\varepsilon)$  as well as  $\hat{f}(\varepsilon)$  for different numbers of anchors. We see there that only a few anchors (i.e., few observations) are required to accurately estimate the localization errors' PDF. Furthermore, from Fig. 9, the estimated PDF approaches the empirical one, as  $N_a$  increases. This gives a sanity check for the proposed nonparametric method.

Nevertheless, in order to derive  $\sigma_{ki}^2$  using this approach, each regular node needs to be aware of all observations. If this is not properly done, it will be very expensive in terms of power consumption, since each anchor would recur to a second broadcast to share its observations with the regular nodes. In order to circumvent this problem, we propose in what follows a power-efficient observation sharing protocol where anchors periodically broadcast their information. In fact, during the first time slot, only the first anchor should broadcast its own information while the  $(N_a - 1)$  other anchors only execute the tasks described in Section IV-A. At the second time slot, the second anchor derives an estimation error observation using the



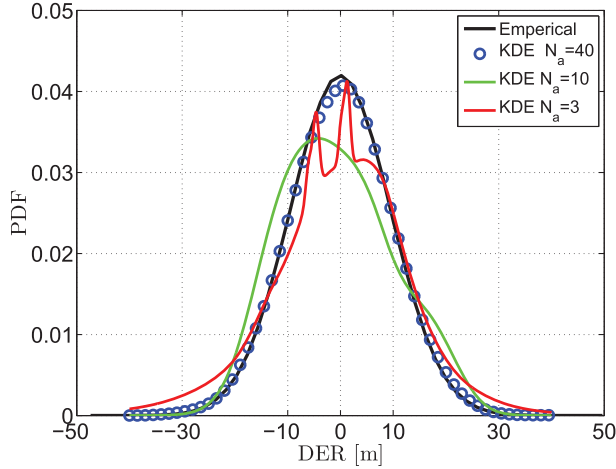


Fig. 9. Estimated DER's PDF using KDE.

information received from the first anchor, adds it to its packet and broadcasts the resulting packet in the network. Upon reception of this information, the rest of anchors derive and store a second observation. Two observations are then available at the third anchor which also broadcasts them in the network. This process will continue until each regular node becomes aware of a sufficient number of observations. Note that if  $N_a$  is large enough so that  $(N_a - 1)$  observations are sufficient to accurately derive the PDF, only two time slots are required. Indeed, after the first time slot,  $(N_a - 1)$  observations are available and can be simultaneously broadcasted by the  $(N_a - 1)$  anchors in the network. In the next section, we will prove that each anchor could transmit few observations without incurring any power cost. Fig. 10 plots the error variance for different node densities. It shows, as expected, that the variance decreases when the node density increases. Beyond a node density threshold of less than 0.1, both the analytical and the non-parametric methods start to yield about the same variance as the empirical one. Furthermore, when  $N_a$  increases, more so at large enough values, the efficiency of the non-parametric method increases even at low node densities. Note that increasing the number of anchors  $N_a$  does not only result in a more accurate variance, but also in a more reliable localization [12].

## VI. PROPOSED ALGORITHM'S IMPLEMENTATION COST

As discussed in Section IV, the Proposed algorithm's implementation requires the  $(i - N_a)$ -th regular node to be able to compute its coordinates' initial guess  $(\hat{x}_i, \hat{y}_i)$  as well as  $\delta_i$  which is used at the position correction step. As discussed above, since these quantities depend solely on the information locally available at the  $(i - N_a)$ -th regular node, their computation does not require any additional overhead or power cost. Furthermore, from (29), this node must perform matrix-inversion operations to the matrices  $\mathbf{Y}\mathbf{Y}^T$  and  $\mathbf{\Gamma}_i^T \mathbf{P}_i^{-1} \mathbf{\Gamma}_i$  in order to derive  $(\hat{x}_i, \hat{y}_i)$  and  $\delta_i$ , respectively. This kind of operations which is often highly computationally demanding may significantly increase the overall cost of the WSN. Nevertheless, since these matrices are 2-by-2, the entries of

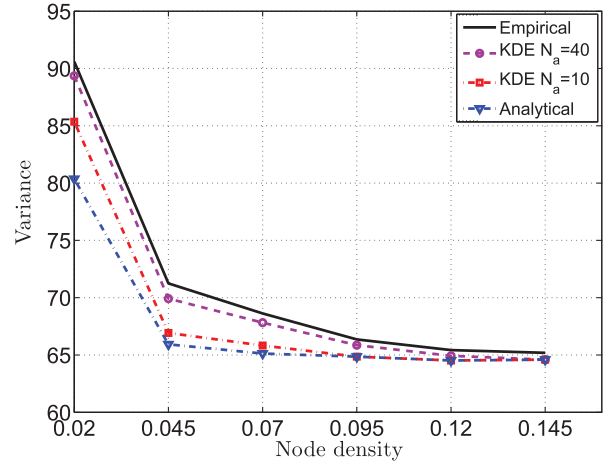


Fig. 10. Global variance for different node densities.

their inverses can be analytically and easily derived using the locally available information at the  $(i - N_a)$ -th regular. This proves that the computation of  $(\hat{x}_i, \hat{y}_i)$  and  $\delta_i$  does not burden neither the implementation complexity of the proposed algorithm nor the overall cost of the WSN. Moreover, some iterations should be repeated, at most 5 times as shown in Fig. 8, to ensure the convergence of the proposed correction mechanism. Knowing that the required power to execute one instruction is in the range of  $10^{-4}$  of the power consumed per transmitted bit [46]–[47], the power needed to execute this mechanism is then very negligible with respect to the overall power consumed by each node. On the other hand, as discussed in Sections IV and V, the proposed algorithm's implementation requires that each node transmits, upon reception a message from an anchor, its transmission capability and variance besides to the latter's coordinates and the distance between the two nodes. This results in additional few bits, with respect to the existent algorithms, thereby causing an additional power cost. We will shortly see below that this cost could be easily avoided.

Let  $p_i$  be the available power at the  $i$ -th node,  $b_i$  be the length in bits of the original packet sent when the existing algorithms are implemented (i.e., packet includes only the anchor's coordinates and its distance to the  $i$ -th node), and  $a_i$  be the cost in bits if  $Tc_i$  and  $\sigma_i^2$  are added to the packet. If the power  $p_i$  allows the  $i$ -th node to transmit  $b_i$  bits over a  $Tc_i$  coverage distance, this power will also allow the latter node to transmit  $b_i + a_i$  bits but over a coverage distance  $\tilde{T}c_i < Tc_i$ , where  $\tilde{T}c_i$  is the new transmission capability of the  $i$ -th node. Since no matter are the transmission capabilities of the  $i$ -th node and the previous intermediate node, this node is always able to compute the EHP, the fact that  $Tc_i$  decreases to  $\tilde{T}c_i$  does not affect the performance of the proposed localization algorithm. Therefore, the additional bits  $a_i$  could be broadcasted without any additional power cost.

All the above discussion proves that the proposed localization algorithm can be implemented at a low cost. Furthermore, since it complies with the heterogeneous nature of WSNs and, further, is power efficient, it could easily find application in EH-WSNs where the power is considered as a scarce resource.

TABLE I  
SIMULATION PARAMETERS

Parameter	Value
$\lambda$	0.02 : 0.025 : 0.145
Transmission capabilities	5 – 30 m
$S$	$10^4 m^2$
$N_a$	20

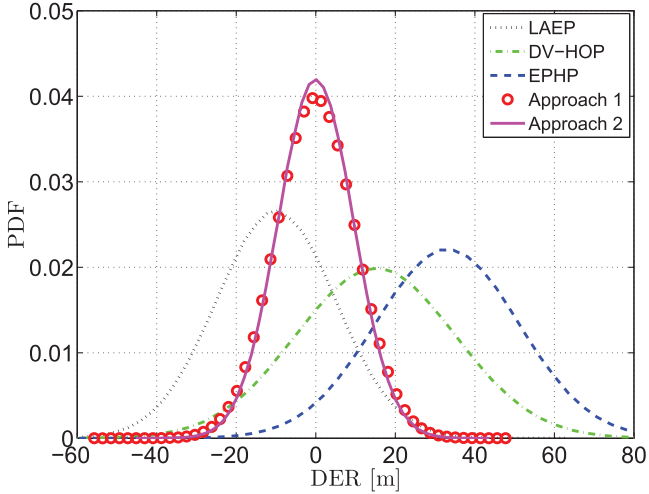


Fig. 11. Empirical PDFs of the DERs achieved by different localization algorithms.

## VII. SIMULATIONS RESULTS

In this section, we evaluate the performance of the proposed algorithm in terms of localization accuracy by simulations using Matlab. These simulations are conducted to compare, under the same network settings, the proposed algorithm with some of the best representative localization algorithms currently available in the literature, i.e., DV-Hop [12], LAEP [23] and EPHP [24]. All simulation results are obtained by averaging over 100 trials. In the simulations, nodes are uniformly deployed in a 2-D square area  $S = 100 \times 100 m^2$ . We always assume that  $T_{c_i} \neq T_{c_j}$  if  $i \neq j$  and that all transmission capabilities are set between 5 and 30 meters, except in Fig. 12(b) where the transmission capability  $T_c = 20$  meters is the same across the network (i.e., homogenous WSN). We also assume that the number of anchors  $N_a$  is set to 20. All simulation parameters are summarized in Table I.

As a performance metric, we propose to adopt both the distance DER and the normalized root mean square error (NRMSE) which is defined as and

$$\text{NRMSE} = \frac{1}{N_u} \sum_{i=1}^{N_u} \frac{\sqrt{(x_i - \hat{x}_i)^2 + (y_i - \hat{y}_i)^2}}{T_{c_i}}. \quad (40)$$

Fig. 11 illustrates the empirical DER's PDF achieved by our proposed localization algorithm as well as those achieved by other well-known algorithms. Since these localization algorithms exploit the distance between each regular node and all anchors to estimate the coordinates of the latter, the better is the distance estimation, the more accurate are these localization algorithms. As can be shown from this figure, when using

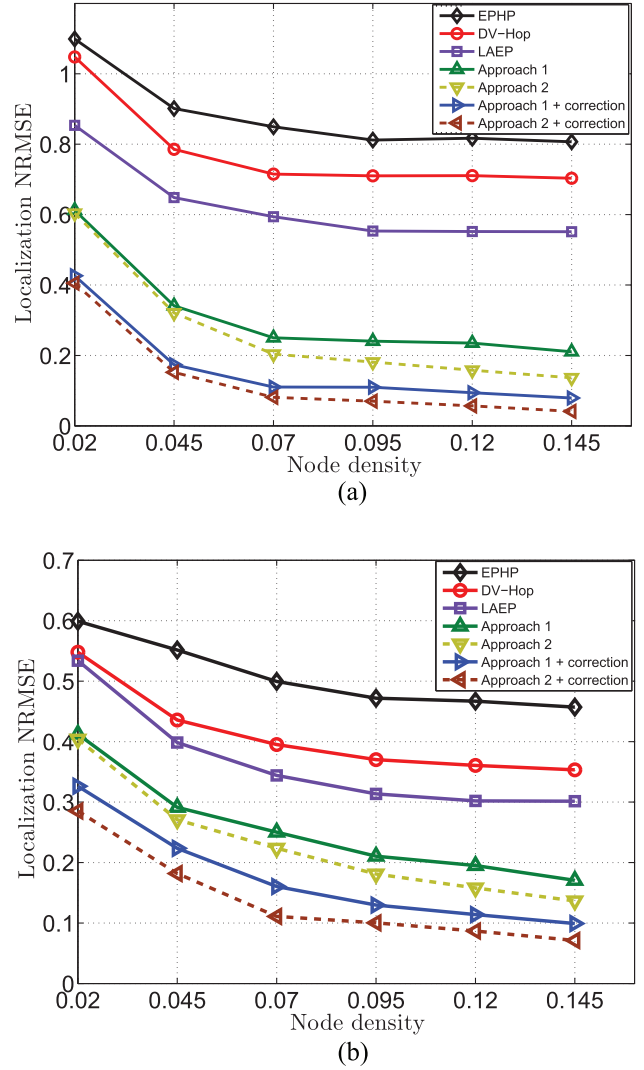


Fig. 12. Localization NRMSE vs. node density in: (a) Heterogenous and (b) Homogenous WSN.

Approaches 1 or 2, we are able to achieve a narrower PDF centered around 0, thereby offering unbiased and far-more accurate distance estimation. This is expected since in contrast to the previous works, both Approaches 1 and 2 take into account the fact that different transmission capabilities may coexist as it is the case in HWSNs.

Fig. 12 plots the localization NRMSE achieved by DV-Hop, EPHP, LAEP and the proposed algorithm for different node densities  $\lambda$  in (a) HWSN and (b) Homogenous WSN. From Fig. 12(a), the proposed algorithm, with or without localization correction, always outperforms its counterparts. Indeed, our proposed algorithm turns out to be until about two, three and four times more accurate than LAEP, DV-Hop, and EPHP, respectively. Furthermore, as can be observed from this figure, the NRMSE achieved by the proposed algorithm significantly decreases when the node density  $\lambda$  increases while those achieved by its counterparts slightly decrease then quickly saturate. This is expected since two conflicting phenomena arise when  $\lambda$  grows large. The first is that the approximation in (30) becomes more realistic and, hence, more accurate localization

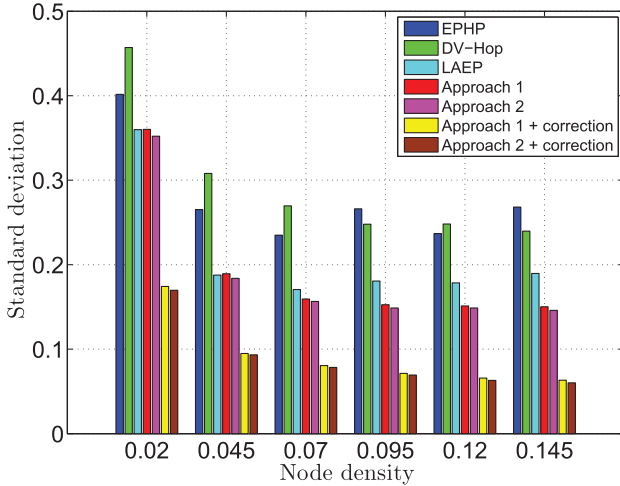


Fig. 13. Standard deviation vs. node density.

is performed. The second is the increase of the number of different transmission capabilities due to the heterogeneous nature of WSNs when the node density increases. Since more different are the transmission capabilities in the network, worse is the accuracy of the former algorithms. This explains why their performance quickly saturates when the node density increases. The proposed algorithm's accuracy, in contrast, increases with  $\lambda$  since it takes into account the difference between the transmission capabilities that is typical of HWSNs. This further proves the efficiency and suitability of the proposed localization algorithm to HWSNs. Moreover, from Fig. 12(b), our algorithm is also the most accurate in homogenous WSNs where the transmission capability is the same across the network. As could be seen from this figure, although the accuracy gaps between the proposed algorithm and its counterparts reduces as expected, the first remains the best algorithm. This is due to the fact that our EHP accounts for the transmission capabilities of the sender and receiver nodes, leading thereby to a more accurate localization. This is in contrast with DV-Hop, EPHP and LAEP whose respective EHPs are derived accounting only for the sender node's transmission capability. The last result further proves the efficiency of our proposed algorithm.

Fig. 13 plots the NRMSE's standard deviation achieved by all localization algorithms. As can be observed from this figure, the one achieved by the proposed algorithm substantially decreases when the node density increases while those achieved by the other algorithms slightly decrease. This is due once again to the fact that the proposed algorithm complies with the heterogeneous nature of the WSNs when the former algorithms do not. Furthermore, the NRMSE standard deviation achieved by the proposed algorithm using either Approach 1 or 2 approaches zero. This means that implementing our algorithm in HWSNs guarantees a very accurate localization for any given realization. This result is very interesting in terms of implementation strategy, since it proves that the result in Fig. 12 becomes more and more meaningful as  $\lambda$  grows large. Fig. 14 illustrates the localization NRMSE's CDF. Using the proposed algorithm, 90% (99.5% with Approach 2) of the regular nodes could estimate their position within almost the fifth of their

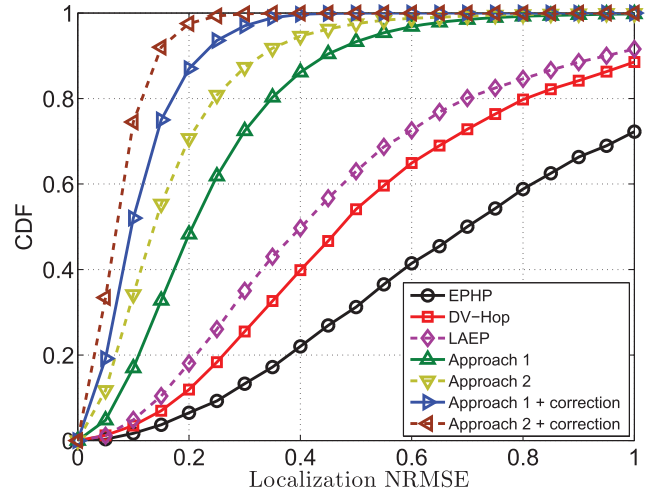
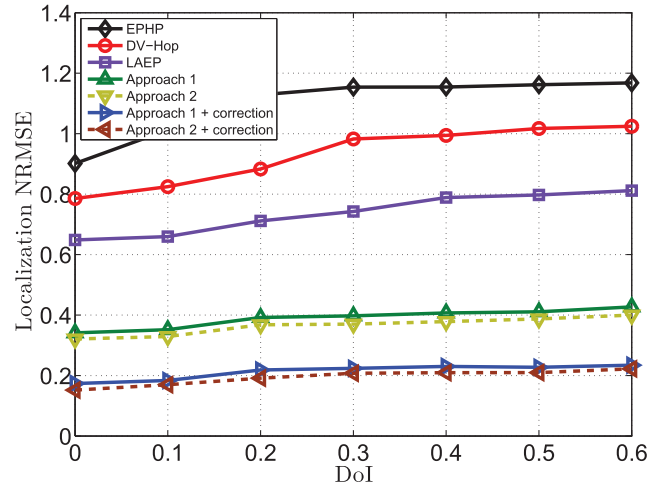


Fig. 14. Localization NRMSE's CDF.

Fig. 15. Localization NRMSE vs. DoI with  $\lambda = 0.045$ .

transmission capabilities. In contrast, 20% of the nodes achieve the same accuracy with LAEP, about 14% with DV-Hop, and only 9% with EPHP. This further proves the efficiency of the proposed localization algorithm.

Fig. 15 plots the localization NRMSE achieved by DV-Hop, EPHP, LAEP and the proposed algorithm versus the degree of irregularity (DoI) of the transmission capabilities, when  $\lambda = 0.045$ . The adopted transmission model in this figure is the same as in [48]. As could be shown from Fig. 15, the accuracy of all algorithms deteriorate, as expected, when DoI increases. However, from this figure, the proposed algorithm still outperforms its counterparts even in more realistic conditions (i.e., practical transmission model). Furthermore, from Fig. 15, our algorithm accuracy slowly deteriorates with DoI, in contrast with its counterparts. This makes it more robust against such a phenomenon and, hence, more suitable for real-world conditions' implementation.

Fig. 16 shows the total number of exchanged packets  $N_{\text{packets}}$  using by the proposed algorithm and its counterparts versus the node density. As could be seen from this figure, the proposed

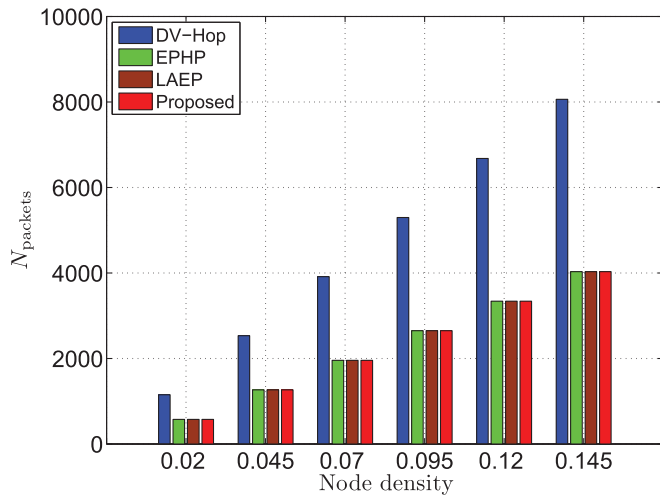


Fig. 16. The total number of exchanged packets  $N_{\text{packets}}$  versus the node density.

algorithm requires the same number of exchanged packets as LAEP and EPHP while it requires the half packets exchanged with DV-Hop. This is expected since the three first are analytical algorithms where the EHP evaluation and, hence, the position estimation are locally performed at each node after the initialization step, without requiring any additional information exchange. This is in contrast with DV-hop whose heuristical nature imposes a second broadcast from the anchors to assist regular nodes' self-localization. This implies that the overall power required by our algorithm to transmit and receive the exchanged packets is the same as that required by LAEP and EPHP while it is the half of that needed by DV-Hop. On the other hand, the additional power cost incurred by the proposed algorithm due to the correction mechanism's instructions is negligible and to the few extra bits in each packet is easily avoidable, as discussed in Section VI. Therefore, our proposed algorithm incurs almost the same power cost as LAEP and EPHP while it incurs the half cost of DV-hop. This proves that although it outperforms in accuracy all its counterparts, the proposed algorithm's implementation almost does not require any additional power cost, thereby highlighting again its superiority.

## VIII. CONCLUSION

In this paper, a novel low-cost localization algorithm which accounts for the heterogeneous nature of WSNs was proposed. Two different approaches were developed to accurately derive the EHP. Using the latter, the proposed algorithm is able to accurately locate the sensor nodes owing to a new low-cost implementation that avoids any additional power consumption. Furthermore, a correction mechanism which complies with the heterogeneous nature of WSNs was developed to further improve localization accuracy without incurring any additional costs. The proposed algorithm, whether applied with or without correction, is shown to outperform in accuracy the most representative WSN localization algorithms.

## REFERENCES

- [1] D. P. Agrawal and Q.-A. Zeng, *Introduction to Wireless and Mobile Systems*, 3rd ed. Stamford, CT, USA: Cengage Learning, 2010.
- [2] S. Zaidi and S. Affes, "Distributed collaborative beamforming in the presence of angular scattering," *IEEE Trans. Commun.*, vol. 62, pp. 1668–1680, May 2014.
- [3] F. Akyildiz, W. Su, Y. Sankarasubramaniam, and E. Cayirci, "A survey on sensor networks," *IEEE Commun. Mag.*, vol. 40, no. 8, pp. 102–114, Aug. 2002.
- [4] J. N. Al-Karaki and A. E. Kamal, "Routing techniques in wireless sensor networks: A survey," *IEEE Wireless Commun.*, vol. 11, no. 6, pp. 6–8, Dec. 2004.
- [5] F. Gustafsson and F. Gunnarsson, "Mobile positioning using wireless networks: Possibilities and fundamental limitations based on available wireless network measurements," *IEEE Signal Process. Mag.*, vol. 22, no. 4, pp. 41–53, Jul. 2005.
- [6] V. Lakafofis and M. M. Tentzeris, "From single-to multihop: The status of wireless localization," *IEEE Microw. Mag.*, vol. 10, no. 7, pp. 34–41, Dec. 2009.
- [7] W. Zhang and G. Cao, "DCTC: Dynamic convoy tree-based collaboration for target tracking in sensor networks," *IEEE Trans. Wireless Commun.*, vol. 3, no. 5, pp. 1689–1701, Sep. 2004.
- [8] H. Ren and M. Q.-H. Meng, "Power adaptive localization algorithm for wireless sensor networks using particle filter," *IEEE Trans. Veh. Technol.*, vol. 58, no. 5, pp. 2498–2508, Jun. 2009.
- [9] J. Rezaaddeh, M. Moradi, A. S. Ismail, and E. Dutkiewicz, "Superior path planning mechanism for mobile Beacon-assisted localization in wireless sensor networks," *IEEE Sens. J.*, vol. 14, no. 9, pp. 3052–3064, May 2014.
- [10] J. Lee, Y. Kim, J. Lee, and S. Kim, "An efficient three-dimensional localization scheme using trilateration in wireless sensor networks," *IEEE Commun. Lett.*, vol. 18, no. 9, pp. 1591–1594, Sep. 2014.
- [11] S. Hong, D. Zhi, S. Dasgupta, and Z. Chunming, "Multiple source localization in wireless sensor networks based on time of arrival measurement," *IEEE Trans. Signal Process.*, vol. 62, no. 8, pp. 1938–1949, Feb. 2014.
- [12] D. Niculescu and B. Nath, "Ad hoc positioning system (APS)," in *Proc. IEEE Global Telecommun. Conf.*, San Antonio, TX, USA, Nov. 25–29, 2001.
- [13] A. Boukerche, H. A. B. F. Oliveira, E. F. Nakamura, and A. A. F. Loureiro, "DV-Loc: A scalable localization protocol using Voronoi diagrams for wireless sensor networks," *IEEE Wireless. Commun. Mag.*, vol. 16, no. 2, pp. 50–55, Apr. 2009.
- [14] L. Gui, T. Val, and A. Wei, "Improving localization accuracy using selective 3-anchor DV-hop algorithm," in *Proc. IEEE Veh. Technol. Conf.*, San Francisco, CA, USA, Sep. 5–8, 2011.
- [15] C. Bettstetter and J. Eberspacher, "Hop distances in homogeneous ad hoc networks," in *Proc. IEEE Veh. Technol. Conf.*, Jeju Island, Korea, Apr. 22–25, 2003.
- [16] D. Ma, M. J. Er, and B. Wang, "Analysis of hop-count-based source-to-destination distance estimation in wireless sensor networks with applications in localization," *IEEE Trans. Veh. Technol.*, vol. 59, no. 6, pp. 2998–3011, Jul. 2010.
- [17] C. Buschmann *et al.*, "Radio propagation-A ware distance estimation based on neighborhood comparison," in *Proc. 4th Eur. Conf. Wireless Sens. Netw.*, The Netherlands, Jan. 29–31, 2007.
- [18] B. Huang, C. Yu, B. D. O. Anderson, and G. Mao, "Estimating distances via connectivity in wireless sensor networks," *Wireless Commun. Mobile Comput.*, vol. 14, no. 5, pp. 541–556, 2014.
- [19] D. Ma, M. J. Er, and B. Wang, "A novel approach toward source-to-sink distance estimation in wireless sensor networks," *IEEE Commun. Lett.*, vol. 14, no. 5, pp. 384–386, May 2010.
- [20] X. Ta, G. Mao, and B. D. Anderson, "On the probability of k-hop connection in wireless sensor networks," *IEEE Commun. Lett.*, vol. 11, no. 9, pp. 662–664, Aug. 2007.
- [21] R. Yates and D. Goodman, *Probability and Stochastic Process*, 2nd ed. Hoboken, NJ, USA: Wiley, 2004.
- [22] X. Ta, G. Mao, and B. D. Anderson, "Evaluation of the probability of k-hop connection in homogeneous wireless sensor networks," in *Proc. IEEE Global Telecommun. Conf.*, Washington, DC, USA, Nov. 26–30, 2007.
- [23] Y. Wang, X. Wang, D. Wang, and D. P. Agrawal, "Range-free localization using expected hop progress in wireless sensor networks," *IEEE Trans. Parallel Distrib. Syst.*, vol. 25, no. 10, pp. 1540–1552, Oct. 2009.
- [24] L. Kleinrock and J. Silvester, "Optimum transmission radii for packet radio networks or why six is a magic number," in *Proc. IEEE Nat. Telecommun. Conf.*, Birmingham, AL, USA, Dec. 4–6, 1978.

- [25] S. Vural and E. Ekici, "On multihop distances in wireless sensor networks with random node locations," *IEEE Trans. Mobile Comput.*, vol. 9, no. 4, pp. 540–552, Apr. 2010.
- [26] A. El Assaf, S. Zaidi, S. Affes, and N. Kandil, "Efficient range-free localization algorithm for randomly distributed wireless sensor networks," in *Proc. IEEE Global Telecommun. Conf.*, Atlanta, GA, USA, Dec. 9–13, 2013.
- [27] M. Haenggi, "On distances in uniformly random networks," *IEEE Trans. Inf. Theory*, vol. 51, no. 10, pp. 3584–3586, Oct. 2005.
- [28] J. C. Kuo and W. Liao, "Hop count distribution of multihop paths in wireless networks with arbitrary node density: Modeling and its applications," *IEEE Trans. Veh. Technol.*, vol. 56, no. 4, pp. 2321–2331, Jul. 2007.
- [29] M. Li and Y. Liu, "Rendered path: Range-free localization in anisotropic sensor networks with holes," *IEEE/ACM Trans. Netw.*, vol. 18, no. 1, pp. 320–332, Feb. 2010.
- [30] A. El Assaf, S. Zaidi, S. Affes, and N. Kandil, "Range-free localization algorithm for anisotropic wireless sensor networks," in *Proc. IEEE Veh. Technol. Conf.*, Vancouver, Canada, Sep. 14–17, 2014.
- [31] B. Xiao, L. Chen, Q. Xiao, and M. Li, "Reliable anchor-based sensor localization in irregular areas," *IEEE Trans. Mobile Comput.*, vol. 9, no. 1, pp. 60–72, Jan. 2010.
- [32] A. El Assaf, S. Zaidi, S. Affes, and N. Kandil, "Accurate nodes localization in anisotropic wireless sensor networks," in *Proc. IEEE Int. Conf. Ubiqu. Wireless Broadband*, Montreal, QC, Canada, Oct. 4–7, 2015.
- [33] Z. Shigeng, C. Jiannong, L.-J. Chen, and C. Daoxu Chen, "Accurate and energy-efficient range-free localization for mobile sensor networks," *IEEE Trans. Mobile Comput.*, vol. 9, no. 6, pp. 897–910, Jun. 2010.
- [34] A. El Assaf, S. Zaidi, S. Affes, and N. Kandil, "Accurate nodes localization in anisotropic wireless sensor networks," *Int. J. Distrib. Sens. Netw.*, vol. 2015, pp. 1–17, Apr. 2015.
- [35] A. El Assaf, S. Zaidi, S. Affes, and N. Kandil, "Accurate sensors localization in underground mines or tunnels," in *Proc. IEEE ICUBW'2015 Workshop Wireless Commun. Underground Confined Environ.*, Montreal, QC, Canada, Oct. 4–7, 2015.
- [36] Q. Xiao, B. Xiao, J. Cao, and J. Wang, "Multihop range-free localization in anisotropic wireless sensor networks: A pattern-driven scheme," *IEEE Trans. Mobile Comput.*, vol. 9, no. 11, pp. 1592–1607, Nov. 2010.
- [37] S. Zaidi, A. El Assaf, S. Affes, and N. Kandil, "Range-free nodes localization in mobile wireless sensor networks," in *Proc. IEEE ICUBW'2015 Workshop V2X Commun. Saf. Autom. Driv. Other Appl.*, Montreal, QC, Canada, Oct. 4–7, 2015.
- [38] A. P. Sample, D. J. Yeager, P. S. Powledge, A. V. Mamishev, and J. R. Smith, "Design of an RFID-based battery-free programmable sensing platform," *IEEE Trans. Instrum. Meas.*, vol. 57, no. 11, pp. 2608–2615, Nov. 2008.
- [39] A. Kansal, J. Hsu, S. Zahedi, and M. B. Srivastava, "Power management in energy harvesting sensor networks," *ACM Trans. Embedded Comput. Syst.*, vol. 6, no. 4, pp. 1–38, Sep. 2007.
- [40] A. El Assaf, S. Zaidi, S. Affes, and N. Kandil, "Efficient node localization in energy-harvesting wireless sensor networks," in *Proc. IEEE ICUBW'2015 Workshop Commun. Energy Harvest. Wireless Power Transfer*, Montreal, QC, Canada, Oct. 4–7, 2015.
- [41] Y. Luo, J. Zhang, and K. B. Letaief, "Optimal scheduling and power allocation for two-hop energy harvesting communication systems," *IEEE Trans. Wireless Commun.*, vol. 12, no. 9, pp. 4729–4741, Sep. 2013.
- [42] S. Sudevalayam and P. Kulkarni, "Energy harvesting sensor nodes: Survey and implications," *IEEE Commun. Surv. Tuts.*, vol. 13, no. 3, pp. 443–461, Third Quart. 2011.
- [43] A. El Assaf, S. Zaidi, S. Affes, and N. Kandil, "Range-free localization algorithm for heterogeneous wireless sensors networks," in *Proc. IEEE Wireless Commun. Netw. Conf.*, Istanbul, Turkey, Apr. 6–9, 2014.
- [44] D. Moltchanov, "Distance distributions in random networks," *Elsevier Ad Hoc Netw.*, vol. 10, no. 6, pp. 1146–1166, Mar. 2012.
- [45] A. El Assaf, S. Zaidi, S. Affes, and N. Kandil, "Cost-effective and accurate nodes localization in heterogeneous wireless sensor networks," in *Proc. IEEE Int. Conf. Commun.*, London, U.K., Jun. 8–12, 2015.
- [46] N. Patwari, J. N. Ash, S. Kyperountas, A. O. Hero, R. L. Moses, and N. S. Correal, "Locating the nodes: Cooperative localization in wireless sensor networks," *IEEE Signal Process. Mag.*, vol. 22, no. 4, pp. 54–69, Jul. 2005.
- [47] J. C. Chen, K. Yao, and R. E. Hudson, "Source localization and beamforming," *IEEE Signal Process. Mag.*, vol. 19, no. 2, pp. 30–39, Mar. 2002.
- [48] G. Zhou, T. He, S. Krishnamurthy, and J. A. Stankovic, "Impact of radio irregularity on wireless sensor networks," in *Proc. ACM MobiSys*, Jun. 2004, pp. 125–138.
- [49] B. W. Silverman, *Density Estimation for Statistics and Data Analysis*, 1st ed. London, U.K.: Chapman and Hall, 1986.

[50] A. R. Webb and K. D. Copsey, *Statistical Pattern Recognition*, 3rd ed. Hoboken, NJ, USA: Wiley, 2011.

[51] A. W. Bowman and A. Azzalini, *Applied Smoothing Techniques for Data Analysis: The Kernel Approach with S-Plus Illustrations: The Kernel Approach with S-Plus Illustrations*. London, U.K.: Oxford Univ. Press, 1997.



**Ahmad El Assaf** received the B.S. degree from the Department of Computer and Telecommunications Networks Engineering, Lebanese University, Saida, Lebanon, and the M.Sc. degree from the University of Quebec in Abitibi-Témiscamingue (UQAT), Val-d'Or, Montreal, QC, Canada, in 2007 and 2012, respectively. He is currently pursuing the Ph.D. degree at INRS-EMT, University of Quebec, Montreal, QC, Canada. His research interests include localization algorithms, machine learning, and wireless sensor networks.



**Slim Zaidi** received the B.Eng. degree in telecommunications from the National Engineering School of Tunis, Tunis, Tunisia, and the M.Sc. degree from INRS-EMT, Université du Québec, Montreal, QC, Canada, both with highest honors, in 2008 and 2011, respectively. He is currently pursuing the Ph.D. degree at INRS-EMT. His research interests include statistical signal and array processing, MIMO, cooperative communications, millimeter wave communications, wireless sensor networks, vehicular ad hoc networks, and cellular networks. He received the

National Grant of Excellence from the Tunisian Government for both the M.Sc. (2009–2010) and the Ph.D. (2011–2013) programs. He also received a Top-Tier Graduate Scholarship from the Natural Sciences and Engineering Research Council (NSERC) of Canada (2013–2015). He had to decline another prestigious Ph.D. Scholarship offered over the same period from the "Fonds de Recherche du Québec Nature et Technologies" (FRQNT). Recently, he received the prestigious FRQNT PDF Grant (2016–2018).



**Sofiene Affes** (SM'04) received the Diplôme d'Ingénieur in telecommunications, and the Ph.D. degree (Hons.) in signal processing, from École Nationale Supérieure des Télécommunications (ENST), Paris, France, in 1992 and 1995, respectively. He was a Research Associate with INRS, Montreal, QC, Canada, until 1997, an Assistant Professor, until 2000, and an Associate Professor, until 2009. Currently, he is a Full Professor and Director of PERWADE, a unique 4M\$ research training program on wireless in Canada involving

27 faculty from eight universities and ten industrial partners. From 2003 to 2013, he was a Canada Research Chair in wireless communications. In 2006, he served as a General Co-Chair of IEEE VTC'2006-Fall, Montreal, QC, Canada. Currently, he is an Associate Editor for the IEEE TRANSACTIONS ON COMMUNICATIONS, the IEEE TRANSACTIONS ON SIGNAL PROCESSING, and the *Wiley Journal on Wireless Communications and Mobile Computing*. From 2007 to 2013, he was an Associate Editor for the IEEE TRANSACTIONS ON WIRELESS COMMUNICATIONS. He is serving now as a General Co-Chair of IEEE ICUBW to be held in Montreal, QC, Canada, in the fall 2015. He has been twice the recipient of a Discovery Accelerator Supplement Award from NSERC, from 2008 to 2011 and from 2013 to 2016. In 2008, he received the IEEE VTC Chair Recognition Award from the IEEE Vehicular Technology Society for exemplary contributions to the success of IEEE VTC.



**Nahi Kandil** has been a Professor with the Engineering School, the University of Quebec, Abitibi-Témiscamingue (UQAT), Val-d'Or, Montreal, QC, Canada, since 2000. He has worked on research dealing with neural networks and their applications to wireless communications and power systems. He is now working mainly with localization and channel modeling in confined areas and mine environments.